ISBN: 978-3-95450-248-6 ISSN: 2673-5490 doi: 10.18429/JACoW-IPAC2025-TUPS054

OPTIMIZATION OF A MULTICHANNEL SOLID STATE PLASMA FOR LASER WAKEFIELD ACCELERATION WITH REALISTIC LASER PARAMETERS USING A BAYESIAN ALGORITHM*

J. Rodríguez-Pérez[1,†], J. Giner-Navarro[1], J. Resta-López[1], H. Aksakal[1,2]
P. Martín-Luna[3], A. Bonatto[4], C. Bontoiu[5], B. Higuera-González[6], G. Xia[6]
[1]ICMUV, Universidad de Valencia, Paterna, Spain
[2]Kahramanmaras Sutcu Imam University, Dep. of Medical Imaging, Turkey
[3]IFIC, CSIC-Universidad de Valencia, Paterna, Spain
[4]Universidade Federal de Ciências da Saúde de Porto Alegre, Porto Alegre, Brazil
[5]University of Liverpool, Liverpool, United Kingdom
[6]University of Manchester, Manchester, United Kingdom

Abstract

Nanostructured plasmas, such as those formed by arrays of carbon nanotubes, offer unprecedented opportunities for advancing laser-plasma interactions in laser wakefield acceleration (LWFA). This study explores the design and optimization of plasmas with hexagonal lattice structures, where the lattice parameters are fine-tuned to tailor the plasma properties and enhance laser coupling. Through fully three-dimensional particle-in-cell (PIC) simulations using WarpX, we model the intricate dynamics of laser pulses interacting with these advanced plasmas, focusing on the formation of effective wakefields. Optimization of the lattice parameters is achieved using Bayesian techniques via the Python library BoTorch, enabling the identification of configurations that maximize wakefield efficiency. These findings provide valuable insights for future experiments at leading laser facilities, such as ELI and VEGA3, highlighting the role of structured plasmas in optimizing laser-plasma interactions for LWFA.

INTRODUCTION

Charged particle acceleration using solid-state high-density nanostructured plasmas has recently gained attention as a promising method for achieving ultra-high acceleration gradients, beam manipulation, and gamma- or X-ray generation, compared to mainstream accelerators such as the LHC [1–8]. Specifically, Laser Wakefield Acceleration (LWFA) uses the wakefield generated by a laser pulse propagating through plasma to accelerate charged particles. Electric field gradients on the order of TV/m can be achieved due to the longitudinal electric field induced by the plasma response. Previous reviews [9] provide detailed discussions on LWFA physics, particularly describing plasma oscillations induced by laser pulses within linear approximations, suitable for low-intensity regimes. For effective coupling in LWFA, the laser pulse length should ideally match the plasma wavelength, $L \simeq \lambda_p$.

To enhance the coupling between the laser pulse and the plasma, and thus improve acceleration efficiency, we introduce a micrometric transverse structure to the plasma consisting of a distribution of carbon nanotubes (CNTs) arrays or nanowires. The plasma is structured as a hexagonal lattice, where CNT arrays are positioned at the lattice nodes, each array characterized by a specific radius r and separated by a distance D, as illustrated in Fig. 1, so that distance between lattice nodes is $2r + D$. This anisotropy channels laser energy along the acceleration axis and modifies plasma response to optimize acceleration and beam shaping [10].

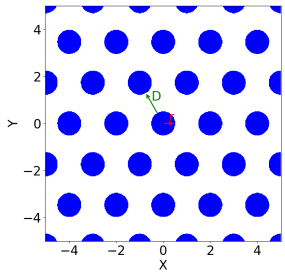

Figure 1: Cross-sectional view of the plasma lattice structure, illustrating CNT arrays or nanowires positioned at the nodes of a hexagonal lattice.

Optimizing the parameters to maximize acceleration gradients within this complex system can be effectively addressed using machine learning techniques, such as the Bayesian optimization implemented in this study. Bayesian optimization algorithms have been successfully applied to enhance the performance of accelerators and their subsystems [11], particularly in the context of plasma wakefield acceleration [12, 13].

SIMULATION SETUP

We used the open-source Particle-in-Cell code WarpX [14] for the simulation of the laser-plasma interaction. We created a fully 3D simulation in which we had a periodic plasma similar to the one shown in Fig. 1, in order to replicate a periodic micrometric structure, where the solid-state plasma is composed by carbon nanotube arrays set in a hexagonal lattice. We control CNT radius and spacing, and thus the structure and effective plasma density. This setup repli-

* Work supported by the Generalitat Valenciana under Grant Agreement CIDEGENT/2019/058.
† juan.rodriguez-perez@uv.es

ISBN: 978-3-95450-248-6 ISSN: 2673-5490 doi: 10.18429/JACoW-IPAC2025-TUPS054

cates a series of CNT arrays that could be grown in a single substrate with a hexagonal pattern, or it also could model some CNT yarns piled up in a similar pattern.

Our simulation box is $128 \times 128 \times 256$ cells, representing a physical domain of $40 \times 40 \times 50\,\mu m^3$, with Perfectly Matched Layer (PML) boundaries. The moving window starts at step 0 at the group velocity of the laser pulse inside the plasma. Simulation lasts 8000 steps (0.488 fs each), totalling 3.905 ps. We set two different plasma species: electrons and carbon ions. The plasma goes from -10 m to 10 m in the x and y directions, and it starts at 0 µm in the z direction, going forward indefinitely. The electrons of the structure are considered to be partially pre-ionized, where all the carbon ions are in a +3 charge state, which have an ionization energy of 64.49 eV. The rest of the laser parameter setup, which is common to all simulation configurations here studied, is shown in Table 1.

Table 1: Set of Laser Parameters

Wavelength, λ_L	800 nm
Intensity, I_L	5×10^{20} W/cm^2
Pulse length, L	λ_p
Phase, ϕ	0

We also have chosen the intensity and wavelength to be similar to the ones used in top laser facilities like ELI and VEGA3.

Parameter Scan

We created a comprehensive database of 108 simulations, systematically scanning CNT densities $n_C \in (10^{23}, 10^{24}, 10^{25}, 10^{26})$ m^{-3}, CNT distances $D \in (0, 0.25, 0.75)$ µm, CNT radii $r \in (0.3, 0.75, 2.0)$ µm, and laser waists $w_0 \in (1.0, 7.5, 15.0)$ µm. This set of parameters captures diverse plasma behaviors under identical laser conditions, including breakup at low, optimal wakefield at intermediate, and absorption at high densities. Additionally, various modes of laser energy channeling were observed, ranging from scenarios of complete electron self-injection into the wakefield to others involving only partial electron acceleration. Such extensive parameter coverage ensures robust Bayesian optimization, facilitating reliable convergence to the global maximum.

BAYESIAN OPTIMIZATION

The Bayesian algorithm used in the optimization of the plasma parameters can be found in the open source Python module BoTorch [15], part of the PyTorch library. The model we trained is called a Multitask Gaussian Process, with a Matérn kernel with $\nu = 5/2$ with an acquisition function of the type logarithmic noisy expected hypervolume improvement.

Metrics

For our model, we used four easily extractable metrics to simplify the training process as much as possible. We trained the model to maximize amplitude and wavelength of longitudinal and transverse wakefields. Maximizing amplitude increases the acceleration gradient, and maximizing the wavelength allows us to have an easier beam injection. These two metrics are adversary as amplitude grows with density $A \propto \sqrt{n}$ while wavelength decreases, $\lambda \propto 1/\sqrt{n}$. This competing metrics are desirable so the model can settle into a stable configuration that maximizes the metrics. If the metrics are not a good representation of the desired behaviour, they can mislead the model. If the metrics represent the behaviour we are looking for accurately, we can expect our model to converge without a problem. As we will see in the next subsection, our metrics are enough to predict additional simulations with similar parameters that show promising results. The model identified self-injection in numerous simulations despite not beeing specifically trained to identify this condition.

Candidate Generation

After training the model, we can ask it to predict some simulation parameters that will maximize the metrics we specified. We need to check if the new suggested simulations really maximize the metrics. These candidates could be used to further train the model and predict better candidates, which suggests a recursive approach.

In our case, we trained with 108 simulations and predicted 23, from which we found at least 3 which show a good convergence towards maximizing hot electron emission. We believe that training the model further with this 23 new predictions could make the number of good predictions increase for the next step.

RESULTS

The Bayesian algorithm produced 23 sets of new parameters to try and simulate. In this paper we will highlight the best two predictions, showing the simulation results obtained with them:

Table 2: Parameters for the Two Candidates

Sim	R **(µm)**	D **(µm)**	n_C $(10^{23}$ m$^{-3})$	w_0 **(µm)**
C.110	0.523	0.0	1.049	10.851
C.122	0.563	0.378	48.972	1.129

Table 3: Metrics for the Two Candidates

Sim	$W_\parallel$ **(V/m)**	$W_\perp$ **(V/m)**	$\lambda_\parallel$ **(µm)**	$\lambda_\perp$ **(µm)**
C.110	1.74×10^{10}	1.72×10^{11}	53.41	4.86
C.122	2.02×10^{9}	1.65×10^{9}	39.99	42.82

In Table 2 we can see the parameters of the two candidate simulations that we will show, while in Table 3 we can see the metrics we obtained for these simulations. We will just

ISBN: 978-3-95450-248-6 ISSN: 2673-5490 doi: 10.18429/JACoW-IPAC2025-TUPS054

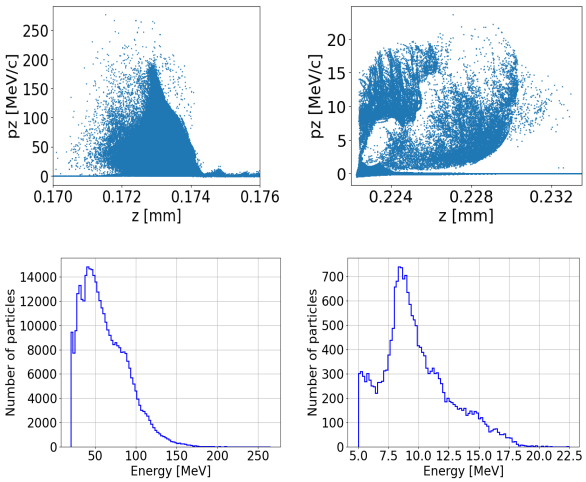

Figure 2: Comparison of longitudinal phase space (top row) and energy spectrum (bottom row) for simulations C.110 at 585.6 fs (left column) and C.122 at 780.8 fs (right column).

show the longitudinal phase space and energy spectrum of hot electrons.

We can see in Fig. 2 the characteristic shape in the longitudinal phase space of electrons accelerating for all the results. Additionally, we observe that the energy spectra exhibit a low-energy peak, and a tail toward higher energy. This indicates electron self-injection followed by acceleration in the wakefield. These plots are shown for the frame of simulation that maximizes the energy. At later times, the bunch of self-injected electrons dephases and gets decelerated. This suggests that maximum acceleration happens in a short length on the order of hundreds of micrometers. Cutting the plasma at the right point would be a very important part of achieving high energies. A quick calculation shows us that C.122 produces an acceleration gradient of 261 GV/m, while C.110 produces approximately 42 GV/m.

This confirms that the model has successfully generalized and is capable of producing optimized simulations. We trained the model to maximize the amplitudes and wavelengths of the wakefields, and it found simulations where these metrics help the electrons self-inject and accelerate to highly relativistic energies. Fig. 3 depicts the transverse distribution of electrons for different simulations and steps. It can be seen in some cases that a great number of electrons get expelled and then self-injected into the wakefield, forming a beam with a high charge density, but it can also be seen that in other cases, the transverse structure helps channel the electrons to form lower energy beams where the charge density is more spread out. This shows the model found different configurations that have electron self-injection.

We can also show a 3D plot of the charge density ρ at the last frame with a mask that shows only regions of high density of negative charge, in our case $\rho < -5 \times 10^4\ \mathrm{C/m^3}$. If we do this for simulation C.110, we obtain a clear proof of acceleration, as shown in Fig. 4, shown by the beam-like shape that can be seen on the right part of the domain.

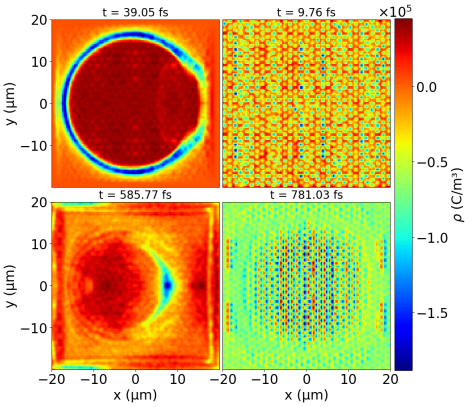

Figure 3: Transverse charge density for simulation 122 (right) at ζ=48.83 μm, and for simulation 110 (left) at ζ=25 μm.

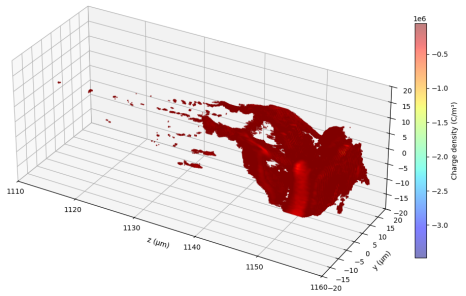

Figure 4: Rho mask for simulation C.110 at 3.905 ps (last frame).

CONCLUSION

We have seen that Bayesian optimization is a capable tool for optimization of parameters in PIC simulations modelling fully 3D nanostructured solid-state plasmas based on carbon nanotube arrays and their interaction with laser. The Bayesian optimization model, trained to maximize the wakefield amplitudes and longer wavelengths successfully predicted input parameter candidates that maximize hot electron emission and acceleration. The model predicted 23 input parameter sets where 3 of them showed energy spectra in the order of MeV in a distance of approximately 1 mm and a good longitudinal phase space. Furthermore, these predicted simulations where not trained to obtain high energy electrons but rather to maximize longitudinal and transverse wakefields. Finding the expected physical behaviour in the simulations means the model is generalizing well. Careful choice of parameter domain and metrics yields informative scans, and better metrics can make the convergence of the model faster and more robust. This algorithm can support experiments at facilities like VEGA3 or ELI, or compare with theoretical models.

ISBN: 978-3-95450-248-6 ISSN: 2673-5490 doi: 10.18429/JACoW-IPAC2025-TUPS054

REFERENCES

[1] X. Zhang *et al.*, "Particle-in-cell simulation of X-ray wakefield acceleration and betatron radiation in nanotubes", *Phys. Rev. Acc. Beams*, vol. 19, p. 101004, 2016. doi:10.1103/PhysRevAccelBeams.19.101004

[2] J. Resta-López *et al.*, "Study of Ultra-High Gradient Acceleration in Carbon Nanotube Arrays", in *Proc. IPAC'18*, Vancouver, Canada, Apr.-May 2018, pp. 599–602. doi:10.18429/JACoW-IPAC2018-TUXGBE2

[3] A. Perera *et al.*, "Towards ultra-high gradient particle acceleration in carbon nanotubes", *J. Phys.: Conf. Ser.*, vol. 1596, p. 012028, 2020. doi:10.1088/1742-6596/1596/1/012028

[4] J. Resta-López *et al.*, "Application of Nanostructures and Metamaterials in Accelerator Physics", in *Proc. IPAC'22*, Bangkok, Thailand, Jun. 2022, pp. 659–662. doi:10.18429/JACoW-IPAC2022-MOPOMS016

[5] A. Bonatto *et al.*, "Exploring ultra-high-intensity wakefields in carbon nanotube arrays: an effective density approach", *Phys. Plasmas*, vol. 30, p. 033105, 2023. doi:10.1063/5.0134960

[6] C. Bontoiu *et al.*, "TeV/m catapult acceleration of electrons in graphene layers", *Sci. Rep.*, vol. 13, p. 1330, 2023. doi:10.1038/s41598-023-28617-w

[7] A. A. Sahai *et al.*, "PetaVolts per meter Plasmonics: introducing extreme nanoscience as a route towards scientific frontiers", *J. Instrum.*, vol. 18, p. P07019, 2023. doi:10.1088/1748-0221/18/07/P07019

[8] M. F. Gilljohann *et al.*, "Channeling acceleration in crystals and nanostructures and studies of solid plasmas: new opportunities", *J. Instrum.*, vol. 18, p. P11008, 2023. doi:10.1088/1748-0221/18/11/P11008

[9] E. Esarey, C. B. Schroeder, W. P. Leemans, "Physics of laser-driven plasma-based electron accelerators", *Rev. Mod. Phys.*, vol. 81, p. 1229, 2009. doi:10.1103/RevModPhys.81.1229

[10] S. Jiang *et al.*, "Effects of front-surface target structures on properties of relativistic laser-plasma electrons", *Phys. Rev. E*, vol. 89, p. 013106, 2014. doi:10.1103/PhysRevE.89.013106

[11] R. Roussel *et al.*, "Bayessian optimization algortihms for accelerator physics", *Phys. Rev. Accel. Beams*, vol. 27, p. 084801, 2024. doi:10.1103/PhysRevAccelBeams.27.084801

[12] H. Jiang *et al.*, "Parallel Bayesian optimization of free-electron lasers based on laser wakefield accelerators", *Plasma Phys. Control. Fusion*, vol. 67, p. 025031, 2025. doi:10.1088/1361-6587/adab1d

[13] B. S. Nunes, A. Bonatto, *et al.*, "Bayesian optimization of laser wakefield acceleration in the self-modulated regime (SM-LWFA) aiming to produce molybdenum-99 via photonuclear reactions", *Phys. Plasmas*, vol. 32, p. 033101, 2025. doi:10.1063/5.0244268

[14] L. Fedeli *et al.*, "Pushing the Frontier in the Design of Laser-Based Electron Accelerators with Groundbreaking Mesh-Refined Particle-In-Cell Simulations on Exascale-Class Supercomputers", in *SC22*, Dallas, TX, USA, 2022. doi:10.1109/SC41404.2022.00008

[15] M. Balandat *et al.*, "BoTorch: A Framework for Efficient Monte-Carlo Bayesian Optimization", in *NeurIPS '20*, 2020. https://proceedings.neurips.cc/paper/2020/hash/f5b1b89d98b7286673128a5fb112cb9a-Abstract.html